ab-plane optical spectra of iodine-intercalated $Bi_{1.9}Pb_{0.1}Sr_2CaCu_2O_{8+\delta}$: Normal and superconducting properties

H. L. Liu* and D. B. Tanner
Department of Physics, University of Florida, Gainesville, Florida 32611

H. Berger and G. Margaritondo
Institute de Physique Appliquée, Ecole Polytechnique Fédérale, CH-1015 Lausanne, Switzerland

(Received 13 July 1998)

We report on the *ab*-plane optical reflectance of an iodine-intercalated $Bi_{1.9}Pb_{0.1}Sr_2CaCu_2O_{8+\delta}$ single crystal in the 80–40 000 cm^{-1} (10 meV–5 eV) frequency range and at temperatures between 10 and 300 K. As compared to the iodine-free $Bi_2Sr_2CaCu_2O_{8+\delta}$, we find that the visible-ultraviolet interband transitions are strongly modified after intercalation. Estimates of the low-frequency spectral weight indicate that there is an increase of hole concentration in the CuO_2 planes. This behavior is a consequence of charge transfer between intercalated iodine atoms and the CuO_2 sheets leading to an ionized iodine species. The *ab*-plane optical conductivity is analyzed in both the one-component and the two-component pictures, suggesting that the intercalated iodine does not have any significant effect on the in-plane scattering rate. In the superconducting state, a sum-rule evaluation finds that the superfluid contains about 25% of the total doping-induced, or nearly 86% of the free-carrier oscillator strength in the normal state. The value of the superconducting penetration depth is estimated to be 1980 Å, slightly larger than the 1860 Å found in iodine-free $Bi_2Sr_2CaCu_2O_{8+\delta}$. [S0163-1829(99)01313-2]

I. INTRODUCTION

It is generally considered that the layered crystal structure of high-T_c superconductors is responsible for their extremely anisotropic behavior, making the physical properties of the cuprate superconductors remarkably anisotropic.[1] For example, one striking feature of these high-T_c materials is their electrical transport anisotropy. The normal-state in-plane resistivity typically varies linearly with temperature, whereas the out-of-plane resistivity almost universally displays semiconducting behavior.[2] In the case of $Bi_2Sr_2CaCu_2O_{8+\delta}$ (Bi-2212), the ratio of the out-of-plane to in-plane resistivities ρ_c/ρ_{ab} can be as high as 10^5. This transport anisotropy[3] is derived from the structural anisotropy. A common view is that the quasi-two-dimensional CuO_2 planes of the cuprate superconductors mainly control the electronic conduction and are intimately related to the superconductivity. In contrast, the influence of the interlayer coupling within the CuO_2 planes on the physical properties is not yet fully understood, although some important models depend on it.[4–6]

Previously, it was reported that iodine can be intercalated between the double Bi-O bilayer of Bi-2212 (IBi-2212) and therefore tune the interlayer coupling strength.[7–10] Structural studies[7–10] of this material reveal that the iodine intercalation expands the *c*-axis unit-cell dimension, whereas it has little effect on the in-plane *a* and *b* parameters. In terms of transport,[10] the effect of iodine intercalation is to depress the superconducting transition temperature T_c by about 10 K. Moreover, the temperature dependence of the resistivity along the *c* axis changes from a semiconducting form to a metalliclike behavior. A general question has been raised to whether the decrease of T_c through the intercalation depends on changes in doped carrier concentration, or is due to a reduced coupling between the superconducting CuO_2 layers. Early reports[8–10] have considered charge transfer associated with the intercalation of iodine to be a negligible effect compared to the change in coupling between the layers. By contrast, an increase in hole density for IBi-2212 was suggested by measurements of Hall effect and x-ray photoemission spectroscopy (XPS).[11,12] Thus, it has been concluded that the observed changes in T_c are caused by the charge transfer from the iodine to the CuO_2 planes. Furthermore, from the pressure dependence of the Hall coefficient in IBi-2212,[13] the hole concentration appears to be situated in the overdoped region of the general T_c vs hole concentration phase diagram. Recently, an angle-resolved ultraviolet photoemission spectroscopy (ARUPS) study[14] of IBi-2212 and O_2 annealed Bi-2212 found that T_c is significantly affected by the interlayer coupling effect rather than solely by hole doping to the CuO_2 planes. Fujiwara *et al.*[15] and Kluge *et al.*[16] have also investigated the effects of iodine intercalation for Y- and Co-substituted Bi-2212. Based on the resistivity and ac susceptibility measurements, they claimed that T_c evolution upon intercalation is likely dependent on both factors: the doped hole concentration and interlayer coupling.

Another question of interest is the valence state of iodine in IBi-2212. The XPS studies[11,12] showed that the iodine is largely in a strongly ionized I^- form but with a small proportion occurring as I^{7+}. According to the pressure dependence of Hall-effect measurements,[13] the valence state of iodine in IBi-2212 is I_3^- molecular anion state. At high pressure, the I_3^- anion probably decomposes as follows: $I_3^- \rightarrow 3I^- + 2p$ (p is a hole). Two Raman studies of IBi-2212 (Refs. 17 and 18) confirmed that the guest iodine is stabilized as a I_3^- anion, acting as an electron acceptor in the host lattice. On the contrary, another Raman-scattering

experiment[19] showed that the intercalated iodine atoms are not ionized and exit as I_2 molecules.

In this paper, we report the *ab*-plane reflectance spectra of an IBi-2212 single crystal in the frequency range from the far-infrared to the near-ultraviolet and at temperatures above and below T_c. Infrared spectroscopy measurements have been proven to be an effective technique for characterizations of high-T_c superconductors.[20,21] Our goal is to determine how the iodine intercalation affects the *ab*-plane optical response of Bi-2212. The results presented here are compared with data for the iodine-free Bi-2212.[22–25] On the basis of the optical data, we will also discuss the origin of the decrease in T_c through intercalation and the valence state of intercalated iodine atoms.

II. EXPERIMENTAL

Single-phase stage-1 IBi-2212 was prepared using the method reported by Xiang *et al.*[7–10] The nominal composition of our host crystal was $Bi_{1.9}Pb_{0.1}Sr_2CaCu_2O_{8+\delta}$. For the most part, such a small amount of Pb doping does not affect the crystal structure of Bi-2212 itself, but does affect the superlattice periodicity along the *b* axis. The dimensions of the sample were about $2\times2\times0.1\,\mathrm{mm}^3$. The superconducting transition determined by a dc magnetization measurement gave a T_c onset 80 K with $\Delta T_c = 4$ K. Characterizations of dc resistivity, x-ray diffraction, low-energy electron diffraction (LEED), XPS, and ARUPS were also performed on similar samples.[14]

The optical reflectance spectra of IBi-2212 were measured for light polarized parallel to the *ab* plane from 80–40 000 cm^{-1} (10 meV–5 eV) and at temperatures between 10 and 300 K. A Bruker IFS 113v Fourier transform spectrometer was used in the far-infrared and mid-infrared regions (80–4000 cm^{-1}), while the near-infrared to near-ultraviolet regions (1000–40 000 cm^{-1}) were covered using a Perkin-Elmer 16U grating spectrometer. Temperature measurements in the whole frequency range were made by using a continuous helium flow cryostat with a calibrated Si-diode thermometer. The 300 K absolute reflectance was calibrated by the data measured with a Zeiss Microscope Photometer system in the range from 5000 to 40 000 cm^{-1}. Moreover, all the spectra are normalized to the same sample coated by a 2000-Å-thick layer of Al to correct the surface scattering loss.

Due to the wide frequency range of our measurements, the optical constants can be estimated by Kramers-Kronig analysis of the reflectance data.[26] Formally, the Kramers-Kronig transformation requires a knowledge of the reflectance spectra at all frequencies from 0 to ∞, and so one needs to extrapolate the reflectance data to energies which the measurements do not cover. At low frequencies the extension was done by modeling the reflectance using the Drude-Lorentz model and using the fitted results to extend the reflectance below the lowest frequency measured in the experiment. Between the highest-frequency data point and 40 eV, the reflectance was merged with the Bi-2212 results of Terasaki *et al.*;[27] beyond this frequency range a free-electron-like behavior of ω^{-4} was used.

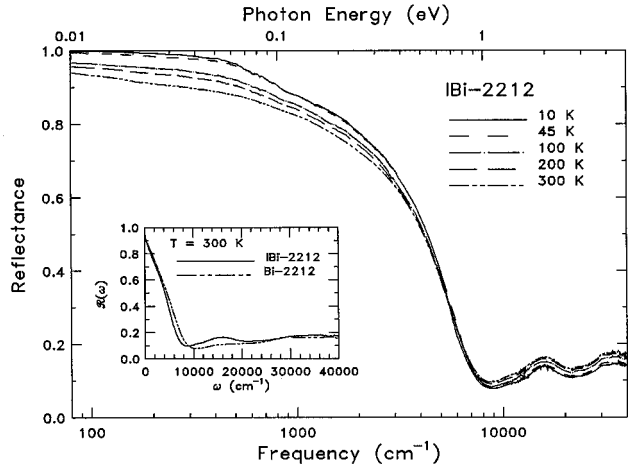

FIG. 1. The *ab*-plane optical reflectance of iodine-intercalated $Bi_{1.9}Pb_{0.1}Sr_2CaCu_2O_{8+\delta}$ in the entire frequency range at different temperatures above and below T_c. For comparison, inset shows the 300 K reflectance spectra of IBi-2212 and iodine-free Bi-2212 (Refs. 23–25).

III. RESULTS AND DISCUSSION

A. Reflectance spectrum

Figure 1 shows the *ab*-plane reflectance for IBi-2212 at several temperatures over the entire measured frequency range. We begin with the room-temperature results. In the infrared region, the reflectance value of IBi-2212 is over 80% for $\omega < 1000\,\mathrm{cm}^{-1}$ at 300 K. As the frequency increases, the reflectance falls off. At higher frequencies, we observe a plasma edge, with a minimum at $\omega \sim 8500\,\mathrm{cm}^{-1}$. For frequencies above the plasma minimum, there are several characteristic bands between 10 000 and 35 000 cm^{-1}. Some of these transitions come from the iodine contributions; there are more clearly seen in the conductivity spectrum discussed later.

The inset of Fig. 1 compares the 300 K reflectance spectrum of IBi-2212 with iodine-free Bi-2212.[23–25] There are three differences between the spectra. First, at low frequencies the reflectance of IBi-2212 is slightly lower than that for Bi-2212. Second, the plasma edge for IBi-2212 occurs at lower frequency than Bi-2212. Third, we find the reflectance is substantially higher for IBi-2212 at frequencies above the plasma minimum. Three new interband transitions in IBi-2212 are evident in this frequency region. One is seen around 17 000 cm^{-1}, the second around 23 000 cm^{-1}, and the last one is at ~34 000 cm^{-1}. As discussed below, these peaks are associated with the iodine intercalation.

When the sample is cooled, there is a substantial temperature dependence in the reflectance up to mid-infrared frequencies, which increases quickly with decreasing temperature until 45 K; changes with temperature below 45 K are much less prominent. At low temperatures, weak phonon modes are also visible in the infrared region. In addition, below T_c we observe the characteristic shoulder in the reflectance at ~500 cm^{-1}, which is a common feature in many cuprate superconductors.[28] The temperature dependence shows the opposite behavior at high frequencies. There is a gradual sharpening and steepening of the plasma edge as the temperature of the sample is lowered. At the same time, the

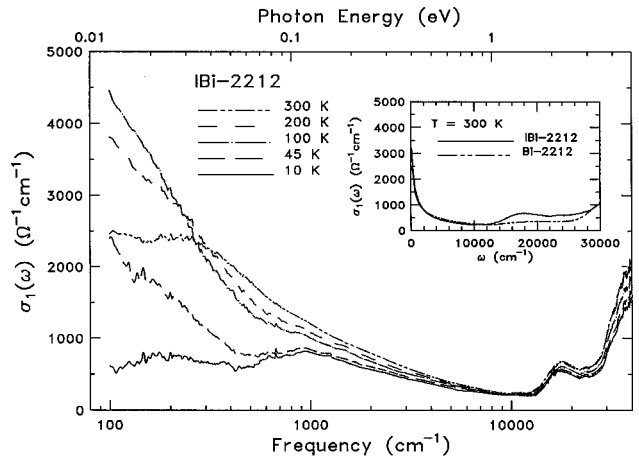

FIG. 2. The real part of the optical conductivity for iodine-intercalated $Bi_{1.9}Pb_{0.1}Sr_2CaCu_2O_{8+\delta}$, calculated through Kramers-Kronig analysis of the reflectance spectra presented in Fig. 1. The inset displays the room temperature $\sigma_1(\omega)$ spectra of IBi-2212 and iodine-free Bi:2212 (Refs. 23–25).

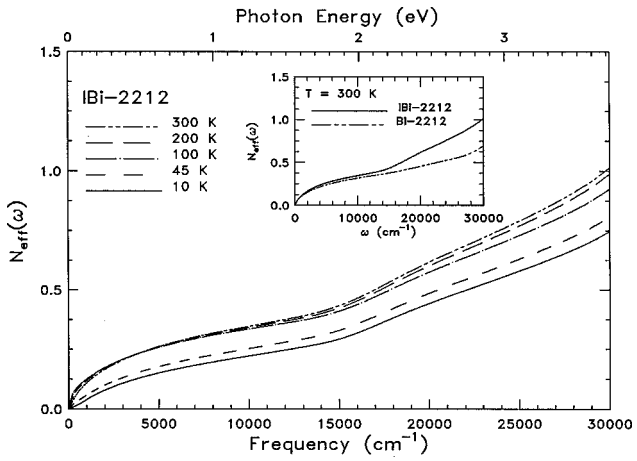

FIG. 3. The effective number of carriers per planar Cu atom as a function of frequency and temperature for iodine-intercalated $Bi_{1.9}Pb_{0.1}Sr_2CaCu_2O_{8+\delta}$, obtained from an integration of the conductivity using Eq. (1). The inset shows the effective carrier numbers for IBi-2212 and iodine free Bi-2212 (Refs. 23–25).

reflectance is reduced (sample becomes less reflecting) for frequencies in the visible and above.

B. Optical conductivity

The real part of the optical conductivity, $\sigma_1(\omega)$, calculated from Kramers-Kronig analysis of the reflectance curves in Fig. 1, is presented in Fig. 2. The temperature dependence of the reflectance gives corresponding changes in $\sigma_1(\omega)$. Above T_c, there is a narrowing and increasing of the far-infrared conductivity as the temperature is lowered. The low-frequency conductivity then decreases dramatically below T_c. The difference in area between the normal-state and superconducting-state conductivities is associated with the condensation of the free carriers into the superfluid.

The conductivity has a modest temperature dependence at mid-infrared frequencies. The mid-infrared conductivity is reduced when cooling the sample from room temperature down to 10 K. We also find that the high-frequency conductivity ($\omega > 10\,000$ cm^{-1}) gradually decreases with decreasing temperature.

To compare the high-frequency conductivity of IBi-2212 with that of the iodine-free Bi-2212,[23–25] we plot the $\sigma_1(\omega)$ spectra for both materials in the inset of Fig. 2. The first interband transition for Bi-2122 ($\omega \sim 19\,000$ cm^{-1}) usually assigns to the charge-transfer band between O $2p$ and Cu $3d$ in the CuO_2 plane. In the case of IBi-2212, the intensity in this range is larger and the central energy occurs at lower frequencies ($\omega \sim 17\,000$ cm^{-1}). The $\sigma_1(\omega)$ spectrum for IBi-2212 has a second peak near 23 000 cm^{-1}, which is not seen for Bi-2212.

This comparison of the characteristic bands in IBi-2212 with those of Bi-2212 suggests that the intercalated iodine contributes to the optical conductivity. We emphasize that new electronic structures observed in the $\sigma_1(\omega)$ of IBi-2212 are not due to either the effects of small amount of Pb doping or the slight difference in oxygen stoichiometry in our sample. The optical reflectance spectrum of Pb doping (43%) looks very similar with that of the iodine-free Bi-2212.[25,29] Moreover, the electronic absorption spectra of I_3^- ions in the CH_2Cl_2 solutions[30] show absorption maxima centered at 17 670, 22 750, 27 500, and 34 040 cm^{-1}. A strong peak near 18 000 cm^{-1} was also observed in the polarized optical spectra of a TCNQ-based organic conductor, (NMe_3H) (I) (TCNQ) (TCNQ:tetracyanoquinodimethane),[31] and has been assigned to the electronic excitation associated with I_3^-. All above features are quite close to those seen in the $\sigma_1(\omega)$ of IBi-2212. This suggests that the iodine is present as I_3^- in IBi-2212. Less good agreement is obtained with the absorption at $\sim$19 230 cm^{-1} of the I_2 molecule.[32] Of course, it is possible both valence states of intercalated iodine atoms exist.

C. Oscillator strength sum rule

In order to give a quantitative basis of conductivity data, we estimate the effective number of carriers (per planar Cu atom) participating in the optical transitions for energy less than $\hbar\omega$. We show in Fig. 3 $N_{\rm eff}(\omega)$, defined as[26]

$$\left[\frac{m}{m^*}\right] N_{\rm eff}(\omega) = \frac{2mV_{\rm cell}}{\pi e^2 N_{\rm Cu}} \int_0^{\omega} \sigma_1(\omega')\, d\omega', \qquad (1)$$

where m^* is the effective mass of the carriers, m is the free-electron mass, $V_{\rm cell}$ is the unit-cell volume, and $N_{\rm Cu}$ is the number of CuO layers per unit cell. Here, we use $N_{\rm Cu} = 2$ for both IBi-2212 and Bi-2212.[33] The effective mass is taken as the free-electron value. The results of evaluation of Eq. (1) in IBi-2212 for various temperatures are presented in Fig. 3. At each temperature, $N_{\rm eff}(\omega)$ at first increases steeply at low frequencies due to the Drude-like band peaked at $\omega = 0$, rises more slowly in the mid-infrared region, and begins to level off near 8000 cm^{-1}. It then rises again above the onset of the charge-transfer band. From the plateau value of the integrated spectral weight at $\sim$8000 cm^{-1}, information on the effective number of the total carriers $N_{\rm tot}$ (per planar Cu atom) in the CuO_2 plane can be obtained. The value of $N_{\rm tot}$ is 0.43 ± 0.03 at room temperature.

There is some variation in the normal-state $N_{\rm eff}(\omega)$ with temperature. As the temperature is reduced, the spectral

weight associated with the free carriers shifts to lower frequencies; this is reflected in the rapid narrowing of low-frequency conductivity with decreasing temperature, shown in Fig. 2. The $N_{\rm eff}(\omega)$ curves in the superconducting state show a reduction of spectral weight in the whole frequency range as compared to the normal-state cases. The area in $\sigma_1(\omega)$ from the superconducting state which appears in the δ function at $\omega=0$ is not included in the numerical integration which yields $N_{\rm eff}(\omega)$. The difference between $N_{\rm eff}(\omega)$ above and below T_c therefore provides a good measure for the spectral weight in the superfluid condensate. We estimate the number of effective carriers per copper in the superfluid $N_s = N_{\rm eff}(100\,{\rm K}) - N_{\rm eff}(10\,{\rm K}) = 0.108 \pm 0.01$.

Turning to the comparison of the room-temperature $N_{\rm eff}(\omega)$ function between IBi-2212 and Bi-2212,[23–25] shown in the inset of Fig. 3, we highlight two characteristic properties involved in the iodine intercalation. First, we obtain the values of $N_{\rm tot}$ to be 0.43 ± 0.03 for IBi-2212, and 0.38 ± 0.03 for Bi-2212. Second, for higher frequencies, the increased oscillator strength due to the electronic transitions associated with the iodine intercalation is readily evident. The larger $N_{\rm tot}$ number in IBi-2212 suggests that the total doping-induced carriers in the CuO_2 planes increase after iodine intercalation. It is less likely that the *ab*-plane spectral weight increase in IBi-2212 is the one in which the Bi-O planes become conducting since the Hall effect and XPS measurements[11–13] also appear to support the fact that the charge transfer occurs from the iodine to the CuO_2 planes. It is important to point out that the difference of carrier concentration in IBi-2212 and iodine-free Bi-2212 is mainly due to iodine intercalation, because the effects of small amount of Pb doping in our sample can be negligible. Analysis of optical conductivity for Pb doped (43%) Bi-2212 gives only 5% increase of hole concentration in the CuO_2 planes as compared to Bi-2212.[25,29]

As was stated above, the valence state of the intercalated iodine has been investigated by several groups.[11,12,17–19] According to our optical results, neutral molecular iodine I_2 alone seems unlikely because it cannot contribute to the increase of carrier density in the CuO_2 planes. Instead, the iodine atoms must be ionized more or less to supply the CuO_2 sheets with about 0.05 holes per CuO_2 unit. The increase of carrier density in the CuO_2 planes is favorable for the decrease in T_c from our optical experiments. Unfortunately, we cannot rule out the effect of interlayer coupling since the change of the *c*-axis resistivity in IBi-2212 (Ref. 10) implies that the interlayer coupling also plays an important role.

D. Quasiparticle scattering rate

To understand better the effect of iodine intercalation on *ab*-plane optical conductivity, we analyze the $\sigma_1(\omega)$ using ''one-component'' and ''two-component'' models. There has been much discussion over the one-component and the two-component pictures to describe the optical conductivity of high-T_c superconductors.[21] In the two-component model, there are two channels of conductivity; (1) a Drude component with a temperature dependent quasiparticle scattering rate, and (2) a broad mid-infrared component that is essentially temperature independent. In contrast, the arbitrary nature of the mid-infrared band in the two-component model has lead to the more general assumption of the one-component, or generalized Drude model, in which the damping rate is frequency dependent.

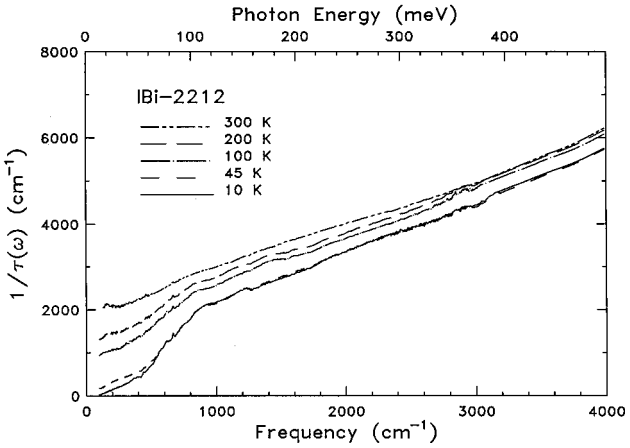

FIG. 4. The temperature-dependent quasiparticle scattering rate $1/\tau(\omega)$ obtained from the generalized Drude model [Eq. (2)] for iodine-intercalated $Bi_{1.9}Pb_{0.1}Sr_2CaCu_2O_{8+\delta}$.

1. One-component model

We first make the generalized Drude analysis, in which the dielectric function is written as

$$\epsilon(\omega) = \epsilon_\infty - \frac{\omega_p^2}{\omega[m^*(\omega)/m][\omega + i/\tau^*(\omega)]}. \qquad (2)$$

Here ϵ_∞ is background dielectric constant associated with the charge-transfer and higher frequency contributions, $m^*(\omega)$ and $1/\tau^*(\omega)$ are the frequency-dependent (renormalized) mass and scattering rate of the charge carriers, and ω_p (the bare plasma frequency) $= \sqrt{4\pi n e^2/m^*}$, with n the carrier density. Another quantity $1/\tau(\omega) = (m^*/m)1/\tau^*(\omega)$ represents the unrenormalized quasiparticle scattering rate. For IBi-2212, we determine the values of $\epsilon_\infty = 4.8$ by fitting the 300 K reflectance using a Drude-Lorentz model, and $\omega_p = 18\,300\,{\rm cm}^{-1}$ from integrating conductivity up to the charge-transfer band in the sum-rule analysis [Eq. (1)]. Figure 4 shows the frequency dependent scattering rate $1/\tau(\omega)$ of IBi-2212 for several temperatures. A linearity comes out for $800\,{\rm cm}^{-1} \leqslant \omega \leqslant 4000\,{\rm cm}^{-1}$ at temperatures above and below T_c. This linear frequency dependence has been seen previously in the scattering rate of the cuprates at doping level ranging from lightly underdoped, optimally doped, to overdoped.[34] Indeed, the temperature variation in the high-frequency $1/\tau(\omega)$ of IBi-2212 is similar to that of some overdoped cuprates.[34] Interestingly, below 800 $\rm cm^{-1}$ the scattering rate falls faster than linearly and a threshold structure becomes more evident at lower temperatures. Such behavior was also observed in many underdoped cuprates where a distinct suppression of $1/\tau(\omega)$ develops below a characteristic energy (the pseudogap state) at $T > T_c$.[34]

For comparison, we use an expression for the dielectric function based on the marginal Fermi-liquid theory (MFI)[35,36] and the nested Fermi-liquid theory (NFL).[37,38] The dielectric function in their theories can be written as

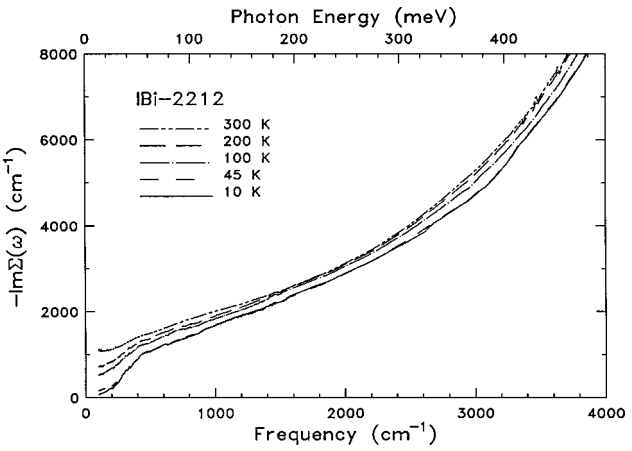

FIG. 5. The imaginary part of the self-energy $-\mathrm{Im}\,\Sigma(\omega)$ for iodine-intercalated $Bi_{1.9}Pb_{0.1}Sr_2CaCu_2O_{8+\delta}$ obtained from the marginal Fermi-liquid theory [Eq. (3)] at several temperatures.

$$\epsilon(\omega)=\epsilon_\infty-\frac{\omega_p^2}{\omega[\omega-2\Sigma(\omega/2)]}, \tag{3}$$

where the factors of 2 arise because quasiparticle excitations come in pairs. The quantity Σ represents the quasiparticle self-energy of the charge carriers and the imaginary part of Σ (essentially the scattering rate) is given by

$$-\mathrm{Im}\,\Sigma(\omega)\sim\begin{cases}\pi^2\lambda_T T, & \omega<T\\ \pi\lambda_\omega\omega, & \omega>T.\end{cases} \tag{4}$$

Here λ_T or λ_ω is a dimensionless coupling constant. For $\omega<T$ the model predicts a renormalized scattering rate that is linear in temperature, as is expected from the linear temperature dependence in the resistivity that is observed in most copper-oxide superconductors. As ω increases, reaching a value of order of T or higher, a new spectrum of excitations arises. This causes the scattering rate to grow linearly with frequency up to a cutoff frequency ω_c that is introduced in the model. The curves for $-\mathrm{Im}\,\Sigma(\omega)$ of IBi-2212 are shown in Fig. 5. Clearly, the linear behavior of the scattering rate exists only up to $\sim$1500 cm^{-1} at each temperature. This low cutoff frequency has been previously pointed out by Romero *et al.*;[39] the MFL approach is limited to a narrow frequency range below 1000 cm^{-1}. It seems necessary to allow for a second component in the optical conductivity at higher frequencies. According to the MFL prescription, we calculate the slope in the region where $-\mathrm{Im}\,\Sigma(\omega)$ is ω linear at 300 K and find a coupling constant $\lambda_\omega\sim0.34$. As the temperature is reduced, the $-\mathrm{Im}\,\Sigma(\omega)$ is depressed below 400 cm^{-1}. This brings the uncertainty to estimate the linear slope of $-\mathrm{Im}\,\Sigma(\omega)$ at low temperatures. We also notice that the energy scale associated with the threshold structure in the $-\mathrm{Im}\,\Sigma(\omega)$ spectra obtained from the MFL analysis is two times smaller than the value in the $1/\tau(\omega)$ spectra by using the generalized Drude approach, consistent with the fact that the MFL theory assumes the quasiparticle excitations coming in pair while it is purely single quasiparticle excitation in the generalized Drude model.

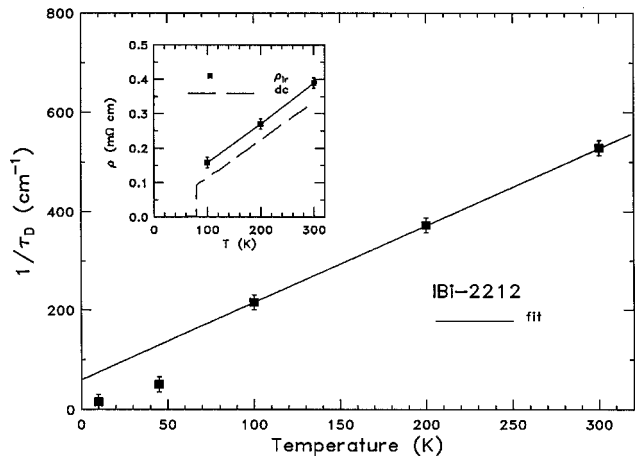

FIG. 6. The zero-frequency scattering rate $1/\tau_D$ (symbols) of the free-carrier contribution from the two-component fit [Eq. (5)] to the optical conductivity of iodine-intercalated $Bi_{1.9}Pb_{0.1}Sr_2CaCu_2O_{8+\delta}$. The straight line shows a linear fit to the temperature dependence of $1/\tau_D$ above T_c. The inset shows the resistivity (symbols) from the infrared measurements and the dc transport data (dashed line) of a similar sample, obtained by Xiang *et al.* (Ref. 10).

2. Two-component picture

We now turn our attention to the two-component model. This is also referred to as the Drude-Lorentz model for the dielectric function:

$$\epsilon(\omega)=-\frac{\omega_{pD}^2}{\omega^2+i\omega/\tau_D}+\sum_{j=1}^{N}\frac{\omega_{pj}^2}{\omega_j^2-\omega^2-i\omega\gamma_j}+\epsilon_\infty, \tag{5}$$

where ω_{pD} and $1/\tau_D$ are the plasma frequency and scattering rate of the Drude component, ω_j, ω_{pj}, and γ_j are the resonant frequency, oscillator strength, and the width of the jth Lorentz contribution. The method of analyzing the data is described in detail in earlier publications.[40–42] We used $N=6$ Lorentz oscillators in the fit, one 80–2000 cm^{-1}, two of these bands fit the mid-infrared spectrum below 8000 cm^{-1} while three are required for the charge transfer and higher bands.

Above T_c, the fits indicate that the Drude contribution of IBi-2212 has a nearly temperature-independent plasma frequency, $\omega_{pD}=8900\pm200\,\mathrm{cm}^{-1}$, which gives for the effective number of free carriers per copper, $N_{\mathrm{Drude}}=0.126\pm0.01$. We also find that the zero-frequency scattering rate $1/\tau_D$ of the free-carrier or Drude contribution has a linear temperature dependence for $T>T_c$, whereas below T_c the scattering rate drops quickly, shown in Fig. 6. Writing $\hbar/\tau_D=2\pi\lambda_D k_B T+\hbar/\tau_0$,[43] with λ_D the dimensionless coupling constant that couples the charge carriers to the temperature-dependent excitations responsible for the scattering and $1/\tau_0$ the zero-temperature value assumed to result from elastic scattering by impurities. We obtain $\lambda_D\sim0.25$ and $1/\tau_0\sim60\,\mathrm{cm}^{-1}$. Using the parameters of Drude plasma frequency $\omega_{pD}\sim8900\,\mathrm{cm}^{-1}$ and the temperature dependence of $1/\tau_D$, the far-infrared resistivity may be calculated as $[\rho_{\mathrm{ir}}=(\omega_{pD}^2\tau_D/60)^{-1}$, in units $\Omega\,\mathrm{cm}]$. This parameter is shown in the inset of Fig. 6, along with the dc transport data of a similar sample.[10] The far-infrared and dc results are in fair agreement, in particular with regard to the linear behav-

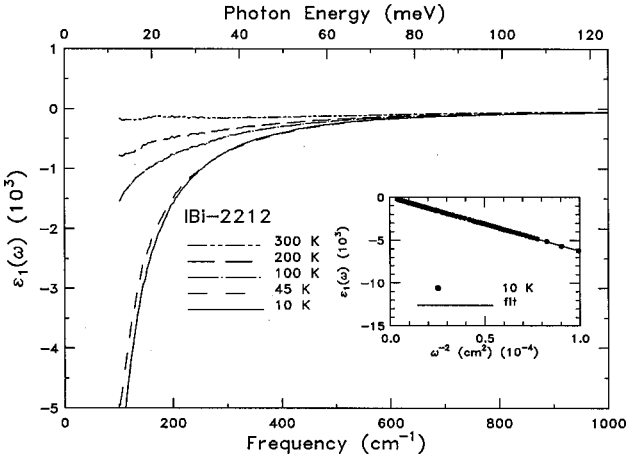

FIG. 7. The real part of the dielectric function $\epsilon_1(\omega)$ (from Kramers-Kronig transformation) at several temperatures for iodine-intercalated $Bi_{1.9}Pb_{0.1}Sr_2CaCu_2O_{8+\delta}$. Inset: a plot of $\epsilon_1(\omega)$ (dashed line) vs ω^{-2} at 10 K. The range of the data shown is 500–100 cm^{-1}. The linear fit is shown by the solid line.

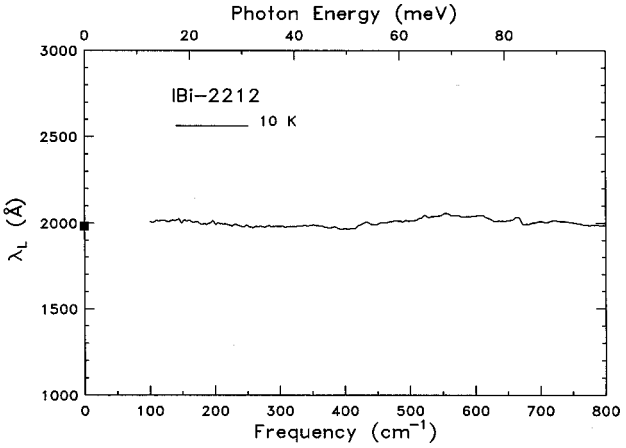

FIG. 8. The frequency-dependent superconducting penetration depth $\lambda_L(\omega)$ of iodine-intercalated $Bi_{1.9}Pb_{0.1}Sr_2CaCu_2O_{8+\delta}$ at 10 K. The value of $\lambda_L(0)$ from the sum-rule analysis is indicated by the symbol.

ior in resistivity with decreasing temperature. There is a discrepancy in the residual resistivity with a larger nonzero intercept for our sample in a linear extrapolation to $T=0$. Additionally, we estimate that the mean-free path for IBi-2212 ($l=v_F\tau_D$) is about 50 Å at 100 K, taking the Fermi velocity of Bi-2212 to be $v_F=2\times10^7$ cm/sec (Ref. 44) and using our free-carrier relaxation rate of $1/\tau_D=210\,\mathrm{cm}^{-1}$. This makes $l>\xi_0$ where the coherence length ξ_0 is typically about 10~15 Å, which, together with the small value of λ_D ~0.25, suggests that IBi-2212 behaves like a clean-limit, weak-coupling superconductor.

E. Spectral weight in the condensate

From the sum-rule analysis, we have obtained the effective number of the superconducting carriers per copper for IBi-2212 as $N_s=0.108\pm0.01$. Expressed as the plasma frequency of the condensate $\omega_{pS}=\sqrt{4\pi n_s e^2/m}$ where $n_s=N_s\cdot N_{\mathrm{Cu}}/V_{\mathrm{cell}}$ is superfluid density,[33] this translates to $\omega_{pS}=8300\pm200\,\mathrm{cm}^{-1}$. The equivalent functions $\epsilon_1(\omega)$, $\sigma_2(\omega)$, $[\sigma_2(\omega)=\{\omega[\epsilon_\infty-\epsilon_1(\omega)]/4\pi\}]$ may also be used to give a estimate of the oscillator strength of the superconducting condensate. The real part of the dielectric function at several temperatures above and below T_c is shown below 1000 cm^{-1} in Fig. 7. The negative values of $\epsilon_1(\omega)$ at low frequencies illustrate the metallic behavior of the system (characteristic of free carriers). As the temperature is lowered below T_c, $\epsilon_1(\omega)$ shows a large negative value, indicating that inductive current dominates conduction current in the superconducting state. In a system where all of the normal-state Drude oscillator strength collapse into the superconducting δ function at $\omega=0$, then this δ function gives a contribution to $\epsilon_1(\omega)$ of

$$\epsilon_1(\omega)=\epsilon_\infty-\frac{\omega_{pS}^2}{\omega^2}. \tag{6}$$

Thus the ω^2 component of the very low-frequency $\epsilon_1(\omega)$ measures the superfluid density. The inset of Fig. 7 shows $\epsilon_1(\omega)$ vs ω^{-2} at 10 K. The slope obtained from a linear regression fit gives $\omega_{pS}=8000\pm200\,\mathrm{cm}^{-1}$, which is only slightly smaller than the sum-rule value.

Figure 8 shows the frequency-dependent penetration depth $\lambda_L(\omega)$, defined as $\lambda_L(\omega)=\sqrt{c^2/4\pi\omega\sigma_2(\omega)}$ where c is the light speed and $\sigma_2(\omega)$ the imaginary part of the optical conductivity. It is clear that $\lambda_L(\omega)$ is almost frequency independent at 10 K, suggesting $\sigma_2(\omega)\gg\sigma_1(\omega)$ at low frequencies. The extrapolated zero-frequency value is about 1980 Å, which is a little larger than the 1860 Å estimated for the iodine-free Bi-2212.[25] The penetration depth is also related to the plasma frequency of the condensate, $\lambda_L=c/\omega_{pS}$, so that a $\lambda_L(\omega\to0)=1980$ Å yields $\omega_{pS}=8100\pm200\,\mathrm{cm}^{-1}$, again in good agreement with the sum-rule value.

Finally, we have used finite-frequency sum-rule analysis to obtain the effective number of carriers per planar Cu atom in (1) the low energy region below the charger-transfer band ($N_{\mathrm{tot}}=0.43\pm0.03$), (2) the Drude or free-carrier part from a two-component analysis ($N_{\mathrm{Drude}}=0.126\pm0.01$), and (3) the superconducting condensate ($N_s=0.108\pm0.01$). Considering the superconducting condensate fraction, it is found that the oscillator strength of the superfluid density contains about N_s/N_{tot}~25% of the total doping-induced carriers or near N_s/N_{Drude}~86% of the free-carrier spectral weight in the normal state. These numbers are consistent with the basic clean-limit argument.

IV. SUMMARY

In summary, we report on the *ab*-plane optical reflectance of an iodine-intercalated $Bi_{1.9}Pb_{0.1}Sr_2CaCu_2O_{8+\delta}$ single crystal over a wide frequency range above and below T_c. A clear observation of differences on the visible-ultraviolet interband transitions, compared to the iodine-free crystal, indicates that the intercalation of iodine does affect the in-plane optical response. Based on the conductivity data, we find that upon intercalation the low-frequency spectral weight increases; that is the increase of hole concentration in the CuO_2 planes. This behavior can be understood as due to holes introduced by intercalated iodine in the CuO_2 planes. The iodine is present as ions, most likely as I_3^-.

We also employ both the one-component and the two-component models to the *ab*-plane optical conductivity in order to investigate the effects of iodine intercalation on the quasiparticle scattering rate. Within the framework of the generalized Drude model and marginal Fermi-liquid theory, the appearance of low-frequency suppression in the scattering rate is similar to the behavior of many underdoped cuprates.[34] Interestingly, the temperature variation of the high-frequency part of the scattering rate is close to what occurs in some overdoped cuprates.[34] Alternatively, the zero-frequency scattering rate $1/\tau_D$ from the free-carrier contributions varies linearly with temperature for $T>T_c$ and decreases quickly below T_c. $1/\tau_D$ from the inelastic scattering process puts our sample in the weak-coupling regime ($\lambda_D \sim 0.25$).

In the superconducting state, a superconducting condensate is evident in the low-frequency *ab*-plane optical data; there is a considerable transfer of oscillator strength from the far-infrared region to the δ function response of the superconductor. A sum-rule evaluation finds the superfluid density contains about 25% of the total doping-induced, or nearly 86% of the free-carrier oscillator strength in the normal state. These numbers are consistent with the basic clean-limit argument. The value of the superconducting penetration depth is estimated to be 1980 Å, slightly larger than the 1860 Å found in iodine-free Bi-2212.

ACKNOWLEDGMENT

This work at University of Florida is supported by National Science Foundation Grant No. DMR-9705108.

*Present address: Department of Physics, University of Illinois at Urbana-Champaign, Urbana, IL 61801.

[1] S. L. Cooper and K. E. Gray, in *Physical Properties of High Temperature Superconductors IV*, edited by D. M. Ginsberg (World Scientific, Singapore, 1993), p. 69.

[2] T. Ito, H. Takagi, S. Ishibashi, T. Ido, and S. Uchida, Nature (London) **350**, 596 (1991).

[3] S. Martin, A. T. Fiory, R. M. Fleming, L. F. Schneemeyer, and J. V. Waszczak, Phys. Rev. Lett. **60**, 2194 (1988).

[4] J. M. Wheatley, T. C. Hsu, and P. W. Anderson, Nature (London) **333**, 121 (1988).

[5] J. M. Wheatley, T. C. Hsu, and P. W. Anderson, Phys. Rev. B **37**, 5897 (1988).

[6] P. W. Anderson and Z. Zou, Phys. Rev. Lett. **60**, 132 (1988).

[7] X.-D. Xiang, S. Mckernan, W. A. Vareka, A. Zettl, J. L. Corkill, T. W. Barbee, III, and M. L. Cohen, Nature (London) **348**, 145 (1990).

[8] X.-D. Xiang, W. A. Vareka, A. Zettl, J. L. Corkill, T. W. Barbee, III, M. L. Cohen, N. Kijima, and R. Gronsky, Science **254**, 1487 (1991).

[9] X.-D. Xiang, A. Zettl, W. A. Vareka, J. L. Corkill, T. W. Barbee, III, and M. L. Cohen, Phys. Rev. B **43**, 11 496 (1991).

[10] X.-D. Xiang, W. A. Vareka, A. Zettl, J. L. Corkill, M. L. Cohen, N. Kijima, and R. Gronsky, Phys. Rev. Lett. **68**, 530 (1992).

[11] D. Pooke, K. Kishio, T. Koga, Y. Fukuda, N. Sanada, M. Nagoshi, and K. Yamafuji, Physica C **198**, 349 (1992).

[12] J.-H. Choy, S.-G. Kang, D.-H. Kim, and S.-J. Hwang, J. Solid State Chem. **102**, 284 (1993).

[13] T. Huang, M. Itoh, J. Yu, Y. Inaguma, and T. Nakamura, Phys. Rev. B **49**, 9885 (1994).

[14] J. Ma, P. Alméras, R. J. Kelley, H. Berger, G. Margaritondo, A. Umezawa, M. L. Cohen, and M. Onellion, Physica C **227**, 371 (1994).

[15] A. Fujiwara, Y. Koike, K. Sasaki, M. Mochida, T. Noji, and Y. Saito, Physica C **203**, 411 (1992).

[16] T. Kluge, A. Fujiwara, M. Kato, and Y. Koike, Phys. Rev. B **54**, 86 (1996).

[17] E. Faulques and R. E. Russo, Solid State Commun. **82**, 531 (1992).

[18] J.-H. Choy, S.-G. Kang, D.-H. Kim, and N.-H. Hur, in *Superconducting Materials*, edited by J. Etourneau, J.-B. Torrance, and H. Yamauchi (IITT International, Paris, 1993), p. 335.

[19] C. H. Qiu, S. P. Ahrenkiel, N. Wada, and T. F. Ciszek, Physica C **185**, 825 (1991).

[20] T. Timusk and D. B. Tanner, in *Physical Properties of High Temperature Superconductors I*, edited by D. M. Ginsberg (World Scientific, Singapore, 1989), p. 339.

[21] D. B. Tanner and T. Timusk, in *Physical Properties of High Temperature Superconductors III*, edited by D. M. Ginsberg (World Scientific, 1992), p. 363.

[22] D. B. Romero, C. D. Porter, D. B. Tanner, L. Forró, D. Mandrus, L. Mihaly, G. L. Carr, and G. P. Williams, Phys. Rev. Lett. **68**, 1590 (1992).

[23] M. A. Quijada, D. B. Tanner, R. J. Kelley, and M. Onellion, Z. Phys. B **94**, 255 (1994).

[24] M. A. Quijada, Ph.D. thesis, Department of Physics, University of Florida, 1994.

[25] H. L. Liu, Ph.D. thesis, Department of Physics, University of Florida, 1997.

[26] F. Wooten, in *Optical Properties of Solids* (Academic, New York, 1972).

[27] I. Terasaki, S. Tajima, H. Eisaki, H. Takagi, K. Uchinokura, and S. Uchida, Phys. Rev. B **41**, 865 (1990).

[28] M. Reedyk and T. Timusk, Phys. Rev. Lett. **69**, 2705 (1992).

[29] D. B. Tanner, H. L. Liu, M. A. Quijada, A. Zibold, H. Berger, R. J. Kelly, M. Onellion, F. C. Chou, D. C. Johnston, J. P. Rice, D. M. Ginsberg, and J. T. Markert, Physica B **244**, 1 (1998).

[30] W. Gabes and D. J. Stufkens, Spectrochim. Acta A **30**, 1835 (1974).

[31] M. A. Abkowitz, J. W. Brill, P. M. Chaikin, A. J. Epstein, M. F. Froix, C. H. Griffiths, W. Gunning, A. J. Heeger, W. A. Little, J. S. Miller, M. Novatny, D. B. Tanner, and M. L. Slade, Ann. (N.Y.) Acad. Sci. **313**, 459 (1978).

[32] L. Andrews, E. S. Prochaska, and A. Loewenschuss, Inorg. Chem. **19**, 463 (1980).

[33] We have used the following structural parameters: $5.4\times5.4\times38\,\text{Å}^3$, $Z=4$, $N_{\text{Cu}}=2$ for IBi-2212 and $5.4\times5.4\times30.9\,\text{Å}^3$, $Z=4$, $N_{\text{Cu}}=2$ for Bi-2212.

[34] A. Puchkov, D. N. Bosov, and T. Timusk, J. Phys.: Condens. Matter **8**, 10 049 (1996).

[35] C. M. Varma, P. B. Littlewood, S. Schmitt-rink, E. Abrahams, and A. E. Ruckenstein, Phys. Rev. Lett. **63**, 1996 (1989).

[36] P. B. Littlewood and C. M. Varma, J. Appl. Phys. **69**, 4979 (1991).

[37] A. Virosztek and J. Ruvalds, Phys. Rev. B **42**, 4064 (1990).

[38] C. T. Rieck, W. A. Little, J. Ruvald, and A. Virosztek, Phys. Rev. B **51**, 3772 (1995).
[39] D. B. Romero, C. D. Porter, D. B. Tanner, L. Forró, D. Mandrus, L. Mihaly, G. L. Carr, and G. P. Williams, Solid State Commun. **82**, 183 (1992).
[40] K. Kamarás, S. L. Herr, C. D. Porter, N. Tache, D. B. Tanner, S. Eternad, T. Venkatesan, E. Chase, A. Inam, X. D. Wu, M. S. Hegde, and B. Dutta, Phys. Rev. Lett. **64**, 84 (1990).
[41] D. B. Tanner, D. B. Romero, K. Kamarás, G. L. Carr, L. Forró, D. Mandrus, L. Mihaly, and G. P. Williams, in *High-Temperature Superconductivity*, edited by J. Ashkenazi (Plenum Press, New York, 1991), p. 159.
[42] M. A. Quijada, D. B. Tanner, F. C. Chou, D. C. Johnston, and S.-W. Cheong, Phys. Rev. B **52**, 15 485 (1995).
[43] P. B. Allen, T. P. Beaulac, F. S. Khan, W. H. Butler, F. J. Pinski, and J. C. Swihart, Phys. Rev. B **34**, 4331 (1986).
[44] S. Martin, A. T. Fiory, R. M. Fleming, G. P. Espinosa, and A. S. Cooper, Appl. Phys. Lett. **54**, 72 (1989).